PNA interference mapping demonstrates functional domains in the noncoding RNA *Xist*

Anton Beletskii*†, Young-Kwon Hong*†, John Pehrson‡, Michael Egholm§, and William M. Strauss†¶

†Harvard Institute of Human Genetics, Beth Israel Deaconess Medical Center, Harvard Medical School, 4 Blackfan Circle, Boston, MA 02115; ‡University of Pennsylvania, School of Veterinary Medicine, 3800 Spruce Street, Philadelphia, PA 19104-6046; and §Applied Biosystems, 500 Old Connecticut Path, Framingham, MA 01701

Edited by Stanley M. Gartler, University of Washington, Seattle, WA, and approved May 23, 2001 (received for review April 8, 2001)

The noncoding RNA *Xist* has been shown to be essential for X-chromosome inactivation and to coat the inactive X-chromosome (Xi). Thus, an important question in understanding the formation of Xi is whether the binding reaction of *Xist* is necessary for X-chromosome inactivation. In this article, we demonstrate the failure of X-chromosome silencing if the association of *Xist* with the X-chromosome is inhibited. The chromatin-binding region was functionally mapped and evaluated by using an approach for studying noncoding RNA function in living cells that we call peptide nucleic acid (PNA) interference mapping. In the reported experiments, a single 19-bp antisense cell-permeating PNA targeted against a particular region of *Xist* RNA caused the disruption of the Xi. The association of the Xi with macro-histone H2A is also disturbed by PNA interference mapping.

X-chromosome inactivation is an early developmental process occurring in female mammals to compensate for differences between male and female mammals in dosage of genes residing on the X-chromosome (1, 2, 4). In mammals, dosage compensation is achieved by the transcriptional silencing of genes on one of the two X-chromosomes in females (5). The inactivated X-chromosome (Xi) can be microscopically observed during interphase as a condensed body at the nuclear periphery (6). Moreover, the Xi has been shown to form a nuclear structure termed the macrochromatin body (MCB) known to be enriched for the variant histone, macrohistone H2A (7–10).

On the basis of the study of chromosomal translocations, an interval called the *X inactivation center* (XIC) of the X chromosome has been identified to control the process of inactivation (11, 12). The XIC has been shown to be a complex transcription unit consisting of at least two genes, *Xist* and *Tsix*, which are transcribed off the opposite strands of the same DNA duplex (3, 13–18). Although the function of *Xist* is not known, deletion of the gene leads to failure of X-inactivation, and female knockout mice die near gastrulation (19, 20). In embryonic stem (ES) cells, the *Xist* transcript supplied in an inducible manner by a transgene has been shown to be necessary and sufficient to cause silencing of genes in cis to the transgene (21).

The gene *Xist* is expressed exclusively from the Xi and shows several interesting features. First, both human and mouse *XIST*/*Xist* cDNAs are unusually long, 19.3 and 17.8 kb, respectively (22, 23). Second, the transcript does not seem to encode a protein (3, 16). Third, the *Xist* RNA physically associates with, or "coats," the Xi (3). The silencing was always associated with coating of the chromosome. Two basic questions about *Xist* are: (*i*) How is the coating/binding process related to the structure of the *Xist* RNA; and (*ii*) is the binding reaction of *Xist* to Xi necessary for *Xist* function?

We have developed a technology that we term Peptide Nucleic Acid (PNA)-Interference Mapping (P-IMP) to define in living cells how specific regions of the *Xist* transcript contribute to X-inactivation. These experiments take advantage of the unique properties of PNAs. PNAs are nucleic acid mimics, which contain a pseudopeptide backbone, composed of charge neutral and achiral *N*-(2-aminoethyl) glycine units to which the nucleobases are attached via a methylene carbonyl linker (24–26). PNAs hybridize with high affinity to complementary RNA sequences forming PNA–RNA complexes via Watson–Crick or Hoogsteen binding (26). PNAs are not readily degraded and do not participate in or activate repair or degradative pathways for DNA or RNA, ensuring a very selective range of activity. In addition to the high thermal stability of complexes, PNA–RNA binding is highly sensitive to mismatches (27–30). The PNAs used for P-IMP were conjugated to transportan via a cleavable disulfide linkage. Transportan is a 27-aa chimeric peptide consisting of the N-terminal fragment of the neuropeptide galanin and the membrane-interacting wasp venom peptide mastoparan. The conjugation of PNA to transportan results in rapid energy-independent nonsaturable transport of the PNA–transportan conjugate across the plasma membrane (31–33).

Using P-IMP, we found that a group of PNAs complementary to a distinct repeat region in the first exon of *Xist* completely abolished binding of *Xist* to the X-chromosome and, in so doing, prevented formation of Xi.

Experimental Procedures

RNA folding experiments were performed by using MFOLD software, available at http://mfold2.wustl.edu/~mfold/rna/form1.cgi. Many probable structures were generated by submission of sequence derived from the C region.

For PNA conjugate treatment, we plated 10^4 tetraploid fibroblast cells per well in eight-well Lab-Tek slides (Nalge) 12 h before treatment to allow for cell attachment. PNA conjugates were dissolved in water at 50 μM concentration. The PNA stock was diluted with DMEM with 10% vol/vol Cosmic Calf Serum (HyClone) to a concentration 1 μM. PNA conjugate and medium mixture (0.2 ml) was then added to the cells. Afterward, PNA conjugate treatment slides were cooled on ice and processed for RNA fluorescence *in situ* hybridization (FISH).

Diploid female ES cell (mWS244.6) culture and differentiation were accomplished by standard method (21). Cells (5×10^4 per well) were treated for 6 days with 1 μM PNA in the presence of 10^{-7} M retinoic acid. To maintain high PNA concentration, medium was changed every 12 h. PNAs used are indicated below and in the text.

To perform the TaqMan assay, total RNA was isolated by using Tri-Reagent (Sigma) according to the manufacturer's instructions. Total RNA was treated with 1 unit of RQ-DNase (Promega) per 10 μg of RNA. TaqMan quantitative PCR analysis was performed by using the EZ-RT-PCR Core Reagent from Applied Biosystems. Four hundred nanograms of total

This paper was submitted directly (Track II) to the PNAS office.

Abbreviations: MCB, macrochromatin body; PNA, peptide nucleic acid; P-IMP, PNA Interference Mapping; Xi, the inactive X-chromosome; ES, embryonic stem; FISH, fluorescence *in situ* hybridization; RT-PCR, reverse transcription–PCR; MCB, macrochromatin body; Xa, the active x-chromosome; BAC, bacterial artificial chromosome; Ch, chromosome.

*A.B. and Y.-K.H. contributed equally to this work.

¶To whom reprint requests should be addressed. E-mail: wstrauss@hihg.med.harvard.edu.

The publication costs of this article were defrayed in part by page charge payment. This article must therefore be hereby marked "*advertisement*" in accordance with 18 U.S.C. §1734 solely to indicate this fact..

GENETICS

RNA was used for analysis. A standard curve was obtained by using serial dilutions of the known concentrations of pWS889, the plasmid containing the 3′ end region of *Xist*. Reverse-transcription reactions and quantification were done by using the ABI 7700 Sequence Analyzer (Applied Biosystems). For *Xist*, two different assays were performed at the 5′ and 3′ regions of the transcript; only data for the 3′ assay are presented (see Fig. 3, which is published as supplemental data on the PNAS web site, www.pnas.org), as both of the assays yielded substantially identical results.

Tsix

pWS1049: (GCCAAGGTGTAAGTAGACTAGCCACT) F. primer

pWS1048: (CGTGGCGGTGCAAACTAAA) R. primer

pWS1304: (6FAM-CTCAGCCCGTTCCATTCCTTTG-TATTGTT-TAMRA) TaqMan probe

mouse *Idh1*

pWS1394: (ACCGCATGTACCAGAAAGGG) F. primer

pWS1395: (CTCGGGACCAGGCAAAAAT) R. primer

pWS1396: (6FAM-AGAGACGTCCACCAACCCCATT-GCTT-TAMRA) TaqMan probe

mouse *Dnmt3b*

pWS1397: (CAGGTCTCGGAGACGTCGAG) F. primer

pWS1398: (CTTCCATGAAGTCGACGCTG) R. primer

pWS1399: (6FAM-TCGTCTTCAGCAAGCACGCCATG-TAMRA) TaqMan probe

mouse *Hmg2*

pWS1400: (GGGCAAAATGTCCTCGTACG) F. primer

pWS1401: (CGAGTCGGGATGCTTCTTCT) R. primer

pWS 1402: (6FAM-CAGACCTGCCGCGAGGAGCAC-TAMRA) TaqMan probe

5′ *Xist* assay

pWS1048: (CGTGGCGGTGCAAACTAAA) F. primer

pWS1049: (GCCAAGGTGTAAGTAGACTAGCCACT) R. primer

pWS1304: (6FAM-CTCAGCCCGTTCCATTCCTTTG-TATTGTT-TAMRA) TaqMan probe

3′ *Xist* assay

pWS483: (AACAGTTAGGTCCCGGCTTT) F.primer

pWS831: (CTTTGCTTTTATCCCAGGCA) R. primers

pWS869: (6FAM-TCTGTGTGGAGCTTTGTGAAG-TAMRA) TaqMan probe

RNA-FISH was done according to refs. 22 and 23. RNA-FISH probes: for *Xist*, full length cDNA = pWS1081, and for β-actin, a murine BAC from Genome Systems (St. Louis) (assignment no. 324C19). Histone macroH2A1 immunofluorescent labeling was done according to Costanzi and Pehrson (9).

For actinomycin D treatment, we plated 10^4 cells per well in eight-well Lab-Tek slides (Nalge) 12 h before treatment to allow for cell attachment. Actinomycin D stock was diluted with DMEM with 10% vol/vol Cosmic Calf Serum (HyClone) to a final concentration of either 2.5 or 5 μg/ml. Two hundred microliters of actinomycin D solution was applied to each well. After treatment, slides were cooled on ice and processed for RNA-FISH.

Results

Experimental System. We decided to test whether the structure of Xi could be disrupted in living cells by the administration of sequence-specific PNAs against the *Xist* transcript. PNA–transportan conjugates were selected on the basis of a careful survey of the sequence composition of the *Xist* transcript. Analysis of the cDNA encoding *Xist* shows four repeated regions [Fig. 1 (3)]. This analysis reveals the striking repetitive structure of four distinct regions, termed A, B, C, and D. Further analysis of the C region revealed that it consists of 14 direct repeats of ≈110–120 bases. These repeats contain several conserved regions, in three locations (termed I, II, and III), in which the motif UCAY was observed. The sequence GAGUCAU observed in region II was very conserved from repeat to repeat, with the UCAU being invariant. Similarly, the sequence GAAUUUCACUU in region III was almost invariant throughout the C region.

Table 1. PNA used in this study

5′-sequence	Name	Orientation
Experimental PNA sequences directed against the C-region		
aaattctatgactctggaa	#pWS1246	Antisense
aaattccatgactctgtaa	#pWS1248	Antisense
aaattccatgactctagaa	#pWS1250	Antisense
Experimental PNA sequences directed against the B-region		
ggggcaggggctggggca	#pWS1458	Antisense
Experimental PNA sequences directed against the D-region		
ggagaaatagacacacaaa	#pWS1380	Antisense
Nonspecific control		
cggactaagtccattgc	#pWS1252	Scramble sequence
PNA control: Sense sequences directed against the C-region		
ttccagagtcatagaattt	#pWS1247	Sense
ttacagagtcatggaattt	#pWS1249	Sense
PNA control: 3-bp mismatch on C region		
aaattccacagctctggaa	#pWS1290	Antisense
PNA control: Directed to the 3′ end (used as a cocktail)		
ctgattgttgtcaattttattattc	#pWS1295	Antisense
tttatgcaagaatgttaaac	#pWS1296	Antisense
tcaatttggtctttcgttcctccag	#pWS1284	Antisense

These motifs have been observed in other systems where they are involved in RNA–protein interactions (34–36). Several lines of evidence, including x-ray crystallographic analysis, show that the NOVA2/NOVA1-binding site is UCAY, where Y stands for a pyrimidine. Furthermore, the sequence GAGUCAU was shown to be an optimal binding site for the NOVA2 protein by *in vitro* selection (SELEX) experiments (34–36).

We performed RNA folding experiments with sequences from the C-repeat region, by using the MFOLD software (see *Experimental Procedures*). The modeling experiments revealed that sequences from the C region consistently formed ordered structures, which we call RNA fingers. These RNA fingers have consensus hairpin structures seen in other systems (35).

These observations provided the rational basis for our design of targeting PNA conjugates (Table 1). Antisense PNAs specific for the C region were designed to span region II containing one of the UCAY sites in the RNA fingers. PNA conjugates were also directed at the B and D regions. Also used were the sense version of the *Xist* C-region-binding antisense PNA, an antisense *Xist*-binding PNA with three sequence mismatches, a set of three PNA conjugates (used as a mixture, bind at the *Xist* 3′ end) (22, 37), and a scrambled sequence control.

To determine the effect of PNA on *Xist* binding to Xi, we treated tetraploid male and female murine C57BL/6 dermal fibroblasts with PNA conjugate under optimal conditions (see *Experimental Procedures*). We chose tetraploid cells because a measure of the effect of PNA administration would be more credible if it altered both copies of Xi. The cells were then fixed and hybridized to a full length *Xist* DNA probe to visualize the location of *Xist* RNA by RNA-FISH (see *Experimental Procedures*). The cells were then analyzed under an epifluorescence microscope for the association of *Xist* with Xi.

PNA Conjugates Do Not Alter Steady-State Levels of *Xist* RNA. The first concern in this project was whether antisense PNA-conjugate administration would have an effect on the steady-state levels of RNA. Thus, we first designed experiments to determine the effect of C-region antisense PNA on *Xist* steady-

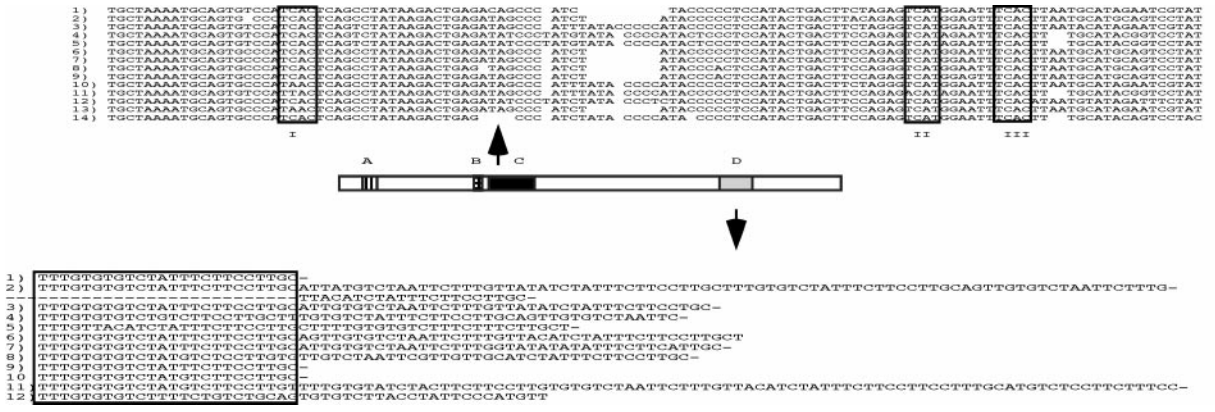

Fig. 1. Description of murine *Xist* repetitive regions used in this study. Schematic line drawing of *Xist.* Repetitive sequence regions are colored and labeled with letters A, B, C, and D (3). The majority of *Xist* transcripts (>90%) do not contain the A region, and thus it was not investigated. Regions C and D are approximately the same size, and antisense oligomers for the C region are directed at the region labeled II and for the D region against the boxed motif.

state RNA levels. Total RNA was isolated from fibroblasts treated with PNA-conjugate for a variety of times. Quantitative reverse transcription–PCR (RT-PCR) was performed by using the TaqMan system (see *Experimental Procedures* and Fig. 3*A*). No difference in *Xist* RNA steady-states levels was observed after PNA treatment.

Specific PNA Conjugates Cause Loss of the *Xist* Body. As steady-state levels of *Xist* did not change after PNA treatment, we wished to determine whether other aspects of *Xist* metabolism might have been altered by treatment. Therefore, RNA-FISH experiments on murine fibroblast cells were performed to identify the presence of the macromolecular complex called the *Xist* body, which has been shown to be congruent with Xi. PNA conjugates directed against the B, C, and D regions were compared. The results of these experiments were tabulated to yield the percentage of cells with *Xist* bodies after different PNA-conjugate treatments (Table 2). Representative microscopic fields are presented in Fig. 2. Cells were treated with the PNA conjugates, as indicated in Fig. 2, Table 2, and notes therein. The results of this experiment showed a clear effect of antisense PNA-conjugates directed to the C region of the *Xist* RNA. PNAs directed against the C region caused the loss of localized *Xist* RNA and the disappearance of the *Xist* body. Antisense PNAs against the B and D regions showed no effect. PNA conjugates, that also had no effect on *Xist* binding, were: C region sense PNA conjugates, scramble sequence PNA conjugate, mismatch C-region antisense PNA conjugate, and a mixture of antisense PNA conjugates directed to the 3′end of *Xist*.

To evaluate the mechanism of action of PNA on *Xist* body loss, we decided to compare the effects of PNA treatment to the effects of the RNA polymerase inhibitor actinomycin D. To evaluate the presence of *Xist* body loss after each treatment, RNA-FISH was performed. The time course of antisense C-region PNA conjugate activity was compared with matched cell cultures treated with actinomycin D. Results were determined by counting percentage of cells with *Xist* bodies. The results of this experiment (see Fig. 3*B*) show that PNA conjugates exhibit a pronounced effect after 18 h of action, with complete activity after 24 h. In contrast, actinomycin D showed complete activity (loss of *Xist* body) in 6 h at 5 μg/ml.

Specific PNA Conjugates Cause Loss of the Histone mH2A Body [Macrochromatin Body (MCB)]. Previously, it has been shown that histone mH2A forms associates with the Xi (9). To establish whether the MCB would disappear after PNA treatment, experiments using the antisense C-region PNA conjugate were performed. PNA conjugate activity was evaluated by Immuno-FISH by using antibodies against the variant histone macrohistone H2A (9). The percentage of cells showing the presence of the macrohistone body was determined as a function of hours of PNA conjugate treatment. The results were plotted with RNA-

Table 2. Numerical results of RNA-FISH experiments depicted in Fig. 2

PNA name	PNA description	No. cells with *Xist* body	No. cells without *Xist* body	Total no. cells	Percent cells with *Xist* body
pWS1246	Xist antisense ''C'' region	12	540	552	2.1
pWS1248	Xist antisense ''C'' region	44	526	570	7.7
pWS1250	Xist antisense ''C'' region	0	505	505	0
pWS1290	Xist antisense ''C'' region with 3bp-mismatch	468	72	546	86.6
pWS1295/1296/1284	Xist antisense to 3′ end	476	53	529	89.9
pWS1249	Xist sense ''C'' region	345	167	512	67.3
pWS1247	Xist sense ''C'' region	427	179	606	70.4
pWS1458	Xist antisense ''B'' region	479	59	538	89.0
pWS1380	Xist antisense ''D'' region	451	53	504	89.5
pWS1252	Scramble sequence	429	106	535	80.1
Female cells no PNA	N/A	501	50	551	90.9
Male cells no PNA	N/A	0	510	510	0

The images presented in Fig. 2 are representative of the response of cells in the experiment. To quantitate the response of cells to PNA-transportan treatment, we counted the cells with *Xist* bodies. The total number of cells counted and number of cells with and without *Xist* bodies, as well as the percentages, are presented. Treatment time was 36 h.

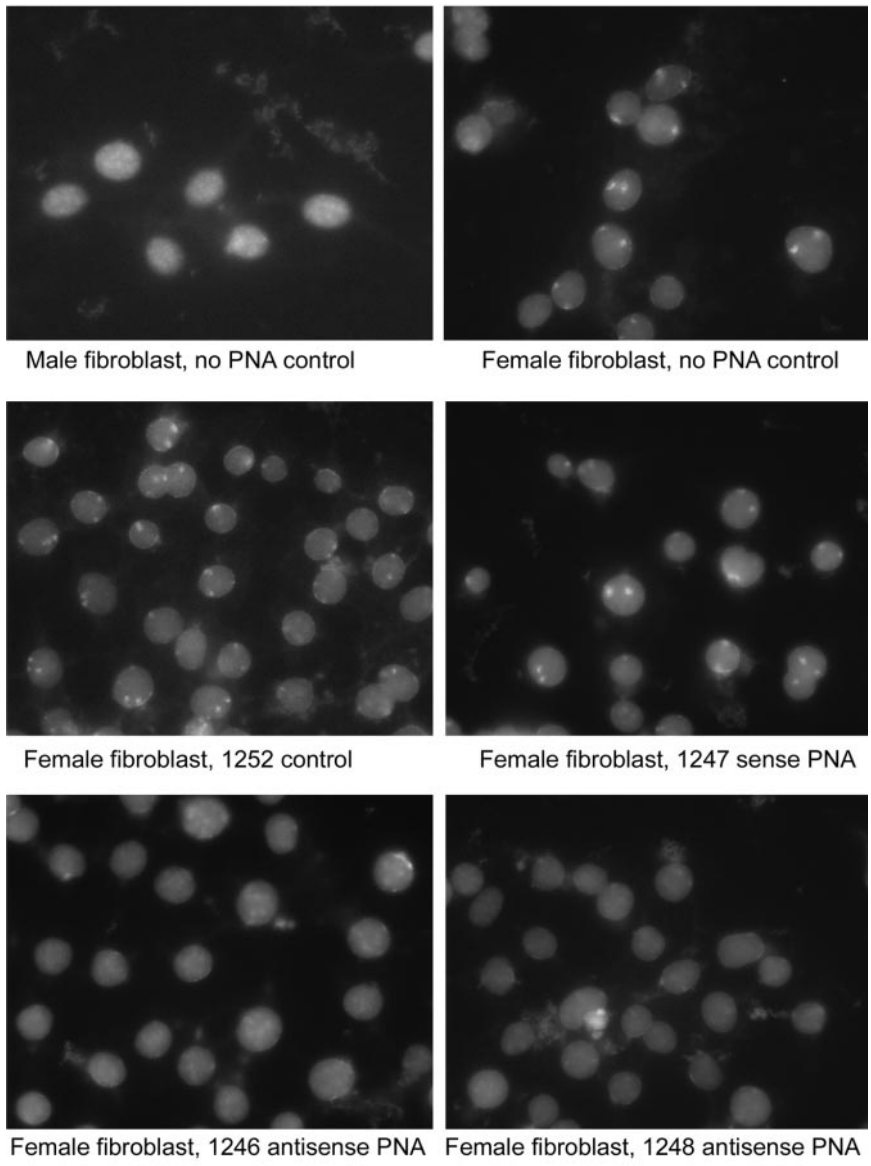

Fig. 2. RNA-FISH of fibroblast cells from various PNA treatments. Female and male fibroblastic cells were treated for 36 h as indicated. After treatment, cells were fixed and processed for RNA-FISH .

FISH time-course results. In these experiments, the MCB was seen to disappear after C-region antisense PNA treatment (see Fig. 3*B*).

***Xist* Must Bind to the X-Chromosome to Function.** To show that *Xist* binding is essential for *Xist* function, diploid female ES cells were differentiated *in vitro*; during the course of differentiation PNA conjugates were added to the media. After the experimental course, samples were processed for analysis.

The effect of PNA administration on the steady-state levels of *Xist* and *Tsix* was measured before or during differentiation. The results of PNA (pWS1248) administration were evaluated by quantitative RT-PCR (TaqMan) for *Xist* and *Tsix*. *Xist* was up-regulated normally in the presence of PNA (see Fig. 3*C*). *Tsix* was down-regulated as previously reported (14, 15) (see Fig. 3*C*). Similarly, PNA administration does not alter expression for genes at autosomal locations. Genes at autosomal locations were evaluated by quantitative RT-PCR. The loci evaluated were *Idh1*:(Chromosome 1), *Dnmt3b*:(Chromosome 2), and *Hmg2*:(Chromosome 8) (see Fig. 3*C*).

PNA-conjugate treatment does not alter the capacity of female ES cells to differentiate normally, as manifested by the appearance of the *Xist* body. Table 3 shows the effect of either

Table 3. Effect of control PNAs on *Xist* body formation in female ES cells

PNA	No signal	*Xist* double dot	*Xist* body	Number nuclei	Percent *Xist* bodies
(−)	17	196	318	531	60
1290	32	207	359	598	60
1252	20	208	307	535	57

We wished to test whether PNA administration by itself could alter the capacity of ES cells to differentiate normally and form *Xist* bodies. We evaluated scrambled sequence (pWS1252) or mismatched sequence (pWS1290) PNAs for their capacity to prevent *Xist* body formation during differentiation of female ES cells (see *Experimental Procedures*). Female ES cells were differentiated and treated with PNA–transportan conjugates for 6 days. The cells were then fixed and assayed for the number of *Xist* bodies by RNA-FISH.

Table 4. Effects of PNA administration on X-linked gene expression as measured by RNA-FISH experiments

	Mecp2 single dot	*Mecp2* double dot	Number nuclei	Percent single dot	Percent double dot	(+) *Xist* bodies	(−) *Xist* bodies	Number nuclei	Percent *Xist* bodies
(−)PNA	288	264	552	52	48	332	220	552	60
(+)PNA	65	415	480	13	87	50	430	480	10

To quantitate the response of cells to PNA–transportan (pWS1248) treatment, we counted the cells with *Xist* bodies, one or two sites of expression for either *Pgk1* or *Mecp2*, as measured by RNA–FISH. The total number of cells counted, number of cells with and without *Xist* bodies, and the number of cells with one or two spots of expression for *Mecp2* are presented.

scramble PNA (pWS1252) or mismatch PNA (pWS1290) on the formation of the *Xist* body. Treated cultures showed the same number of *Xist* bodies as untreated cultures. Further, in Table 3, 60% is a measure of the percentage of female ES cells that have differentiated during the experimental time course of 6 days.

We evaluated the specific effect of *Xist* antisense PNA administration on coating/binding of *Xist* in ES cell culture. Treated and untreated female ES cells at day 6 of differentiation were examined by RNA-FISH. PNA-untreated and differentiated ES cells show the expected *Xist* body and a single site of expression for *Pgk1* and Mecp2 loci. In contrast, PNA-treated and differentiated ES cells do not show a *Xist* body and exhibit two sites of expression for *Pgk1* and loci. When transcription at the murine β-actin locus on Ch 4 was determined by RNA-FISH, no difference between untreated ES cells and ES cells treated with PNA pWS1248 was observed. The RNA-FISH data are tabulated in Tables 3–6. In Tables 3–6, over 500 interphase nuclei from treated and untreated cultures were examined after differentiation and scored for the presence of *Xist* body and the suppression of transcription from either *Pgk1*, *Mecp2*, or β-actin loci.

Discussion

Here we report the first functional demonstration that the large nontranslated RNA, *Xist*, can be organized into functional domains. These studies also confirm that the function of *Xist* is mediated through its binding to X-chromosome. It is also apparent from the kinetic studies in this report that macro histone H2A and *Xist* are intimately associated in a macromolecular complex on Xi.

The process of *Xist*-mediated gene repression observed in X-chromosome inactivation is thought to be a special case of a general developmental pathway for chromatin reorganization directed at transcriptional repression (38, 39). As the nontranslated RNA *Xist* has been shown to be necessary and sufficient to initiate the silencing pathway (21), it is of great interest to discern how the nontranslated RNA *Xist* interacts with the X-chromosome to initiate silencing. One of the most striking qualities of the *Xist* transcript is its localization to the Xi. To make the connection between the structure of *Xist*, its binding to the X-chromosome, and silencing of gene expression, a functional analysis of the *Xist* transcript is vital. Here we report evidence for the existence of a functional domain in *Xist* responsible for *Xist* coating/binding to Xi. We argue that this functional domain appears to be encoded in the repetitive sequence in the large first exon (C region, Fig. 1).

The data presented here definitively demonstrate that C-region antisense PNA-conjugates can alter *Xist* coating/binding. PNA conjugates directed to other regions of *Xist* do not alter its localization. Perfectly matched PNAs against the C region can bind a maximum of seven times; if one or two mismatches are allowed, they can bind a maximum of 14 times. D-region PNA can bind to six perfectly matched target sites, and if mismatches are permitted to at least eight sites. Thus, the amounts of PNA bound to the C and D regions are similar. Nonetheless, antisense PNAs directed against the *Xist* B and D regions, and 3′ end have no effect on *Xist* coating. In addition, the pWS1290 PNA conjugate, which represents a 3-bp mismatch of the active antisense PNA (pWS1248) PNA conjugate, has no effect on coating/binding.

Time-course results show striking differences between the kinetics of PNA action and actinomycin D inhibition on *Xist* body loss. In our experiments, complete loss of *Xist* bodies was observed 6 h after actinomycin D treatment, whereas for PNA treatment, this period was 18–24 h. In the context of no change in *Xist* RNA expression (see Fig. 3), PNA treatment is governed by a slow kinetic path, which remains to be defined. We postulate potential steric factors that might contribute to the inaccessibility of *Xist* to PNA action.

Under conditions where the intracellular levels of steady-state *Xist* RNA do not change (see Fig. 3), the slow step in *Xist* body loss is comparable to the kinetics of MCB loss. The variant histone mH2A has been shown to be associated with the Xi during development (8, 9). Previous attempts at describing the association between the *Xist* body and the MCB required the recombinational loss of the *Xist* gene and subsequent loss of *Xist* expression to measure the association between *Xist* body and the MCB (7). The current kinetic study does not suffer this limitation, as PNA uptake is essentially instantaneous, with high concentrations of PNA available in the nucleus in minutes; further, the rate of change for *Xist* and the MCB can be monitored from the inception of PNA administration. The data presented here would suggest that the binding of *Xist* and the MCB to the Xi are equally destabilized by antisense PNA against the C region. This simultaneous destabilization suggests concerted breakdown of a macromolecular structure by PNA action. The kinetics of dissociation for *Xist* and macrohistone H2A imply that the MCB and *Xist* are in intimate association in the Xi. The loss of the MCB relative to *Xist* is the predicted result if one were to suppose a hierarchical structure where *Xist* represents a foundation on which proteins like mH2A might associate with Xi.

Table 5. Effects of PNA administration on X-linked gene expression as measured by RNA-FISH experiments

	Pgk1 single dot	*Pgk1* double dot	Number nuclei	Percent single dot	Percent double dot	(+) *Xist* bodies	(−) *Xist* bodies	Number nuclei	Percent *Xist* bodies
(−)PNA	241	277	518	46	53	295	223	518	57
(+)PNA	122	396	518	23	76	64	454	518	12

To quantitate the response of cells to PNA–transportan (pWS1248) treatment, we counted the cells with *Xist* bodies, one or two sites of expression for either *Pgk1* or *Mecp2*, as measured by RNA–FISH. The total number of cells counted, number of cells with and without *Xist* bodies, and the number of cells with one or two spots of expression for *Pgk1* are presented.

Table 6. Effect of PNA administration on autosomal expression measured by RNA-FISH

	β-Actin single dot	β-Actin double dot	Number nuclei	Percent single dot	Percent double dot
(−)PNA	16	530	546	3	97
(+)PNA	20	550	570	3	97

PNA conjugate-treated cells were evaluated for alterations in β-actin expression. Actin mRNA expression was evaluated for single or double sites of expression and then tabulated.

Two lines of evidence support the conclusion that PNA activity is caused by the interference with a particular RNA structure. The theoretical folding of the *Xist* RNA by MFOLD algorithm predicts highly stable hairpins. Thus PNA activity against these structures is based on the specificity, not the accessibility, of PNA to *Xist* RNA. Secondly, unique kinetics of MCB disruption by PNA interference is different from actinomycin D time-course, implying that dissociation of *Xist* and the MCB is coupled with, and not attributable to, an alteration in *Xist* metabolism per se.

Coating/binding of *Xist* is necessary for X-inactivation. During female development, a number of changes occur within the XIC. On Xi, *Xist* expression is up-regulated by an unknown mechanism, and *Tsix* expression is silenced. On Xa, expression of both *Xist* and *Tsix* is suppressed. Formally, it has not been proven which of these steps is required for the biochemical process of silencing. Using antisense PNA conjugates that can bind only to the *Xist* transcript, we demonstrate that, despite the ordered progression of developmental stages in differentiating female ES cells, if up-regulated *Xist* cannot bind to the Xi, there is no chromosomal silencing. Thus, the described experiments distinguish between the expression of *Xist* and the correct localization of the transcript with respect to function.

One of the major limitations for analysis of the nuclear compartment and *Xist* function within it has been the lack of a functional technology that would specifically connect DNA sequence-based knowledge to the biochemistry of the nucleus. One of the goals of the present work was to make the connection between *Xist* sequence information and its function. The technology described here, P-IMP, is a functionally based technology to probe the RNA–RNA and RNA–protein interactions that occur in the living cell. P-IMP experiments can be envisaged for a variety of processes that involve nontranslated RNAs, including splicing, telomere formation and maintenance, gene imprinting, and chromatin-mediated gene silencing. It will be exciting to envisage a high-throughput functional genomic analysis of the nuclear compartment by P-IMP.

We thank Ralph A. Casale and Eric G. Anderson for their dedication and skill in the preparation of the PNA conjugates. We acknowledge the support of U.S. Army Prostate Cancer Research Award DAMD17–99-1–9032 and National Institutes of Health Grants R21 CA81732 and RO1 GM61079 (to W.M.S.).

1. Brockdorff, N. (1998) *Curr. Opin. Genet. Dev.* **8,** 328–333.
2. Brockdorff, N. & Duthie, S. M. (1998) *Cell Mol. Life Sci.* **54,** 104–112.
3. Brown, C. J., Hendrich, B. D., Rupert, J. L., Lafreneire, R. G., Xing, Y., Lawrence, J. & Willard, H. F. (1992) *Cell* **71,** 527–542.
4. Lyon, M. F. (1961) *Nature (London)* **190,** 372–373.
5. Gartler, S. M., Chen, S. H., Fialkow, P. J., Giblett, E. R. & Singh, S. (1972) *Nat. New Biol.* **236,** 149–150.
6. Barr, M. L. & Bertram, E. G. (1949) *Nature (London)* **163,** 676–677.
7. Csankovszki, G., Panning, B., Bates, B., Pehrson, J. R. & Jaenisch, R. (1999) *Nat. Genet.* **22,** 323–324.
8. Mermoud, J. E., Costanzi, C., Pehrson, J. R. & Brockdorff, N. (1999) *J. Cell Biol.* **147,** 1399–1408.
9. Costanzi, C. & Pehrson, J. R. (1998) *Nature (London)* **393,** 599–601.
10. Rasmussen, T. P., Mastrangelo, M. A., Eden, A., Pehrson, J. R. & Jaenisch, R. (2000) *J. Cell Biol.* **150,** 1189–1198.
11. Russell, L. B. & Mongomery, C. S. (1965) *Genetics* **52,** 470–471.
12. Russell, L. B. (1963) *Science* **140,** 976–978.
13. Lee, J. T., Strauss, W. M., Dausman, J. A. & Jaenisch, R. (1996) *Cell* **86,** 83–94.
14. Lee, J. T., Davidow, L. S. & Warshawsky, D. (1999) *Nat. Genet.* **21,** 400–404.
15. Lee, J. T. & Lu, N. (1999) *Cell* **99,** 47–57.
16. Brockdorff, N., Ashworth, A., Kay, G. F., McCabe, V. M., Norris, D. P., Cooper, P. J., Swift, S. & Rastan, S. (1992) *Cell* **71,** 515–526.
17. Borsani, G., Tonlorenzi, R., Simmler, M. C., Dandolo, L., Arnaud, D., Capra, V., Grompe, M., Pizzuti, A., Muzny, D. & Lawrence, C. (1991) *Nature (London)* **351,** 325–329.
18. Brown, C. J., Ballabio, A., Rupert, J. L., Lafreniere, R. G., Grompe, M., Tonorenzi, R. & Willard, W. F. (1991) *Nature (London)* **349,** 38–44.
19. Marahrens, Y., Panning, B., Dausman, J., Strauss, W. & Jaenisch, R. (1997) *Genes Dev.* **11,** 156–166.
20. Penny, G. D., Kay, G. F., Sheardown, S. A., Rastan, S. & Brockdorff, N. (1996) *Nature (London)* **379,** 131–137.
21. Wutz, A. & Jaenisch, R. (2000) *Mol. Cell.* **5,** 695–705.
22. Hong, Y. K., Ontiveros, S. D., Chen, C. & Strauss, W. M. (1999) *Proc. Natl. Acad. Sci. USA* **96,** 6829–6834.
23. Hong, Y. K., Ontiveros, S. D. & Strauss, W. M. (2000) *Mamm. Genome* **11,** 220–224.
24. Nielsen, P. E., Egholm, M., Berg, R. H. & Buchardt, O. (1991) *Science* **254,** 1497–1500.
25. Egholm, M., Buchardt.O., Nielsen, P. E. & Berg, R. H. (1992) *J. Am. Chem. Soc.* **114,** 1895–1897.
26. Egholm, M., Buchardt, O., Christensen, L., Behrens, C., Freier, S. M., Driver, D. A., Gerg, R. H., Kim, S. K., Norden, B. & Nielsen, P. E. (1993) *Nature (London)* **365,** 566–568.
27. Verheijen, J. C., Van der Marel, G. A., Van Boom, J. H., Bayly, S. F., Player, M. R. & Torrence, P. F. (1999) *Bioorg. Med. Chem.* **7,** 449–455.
28. Bonham, M. A., Trown, S., Boyd, A. L., Brown, P. H., Bruckenstein, D. A., Hanvey, J. C., Thomson, S. A., Pipe, A., Hassman, F., Bisi, J. E., *et al.* (1995) *Nucleic Acids Res.* **23,** 1197–1203.
29. Brewer, G. & Ross, J. (1989) *Mol. Cell. Biol.* **9,** 1996–2006.
30. Uhlmann, E. (1998) *Biol. Chem.* **379,** 1045–1052.
31. Pooga, M., Lindgren, M., Hallbrink, M., Brakenhielm, E. & Langel, U. (1998) *Ann. N.Y. Acad. Sci.* **863,** 450–453.
32. Pooga, M., Soomets, U., Hallbrink, M., Valkna, A., Saar, K., Rezaei, K., Kahl, U., Hao, J. X., Xu, X. J., Wiesenfeld-Hallin, Z., *et al.* (1998) *Nat. Biotechnol.* **16,** 857–861.
33. Pooga, M., Hallbrink, M., Zorko, M. & Langel, U. (1998) *FASEB J.* **12,** 67–77.
34. Jensen, K. B., Musunuru, K., Lewis, H. A., Burley, S. K. & Darnell, R. B. (2000) *Proc. Natl. Acad. Sci. USA* **97,** 5740–5745. (First Published May 16, 2000; 10.1073/pnas.090553997)
35. Lewis, H. A., Chen, H., Edo, C., Buckanovich, R. J., Yang, Y. Y., Musunuru, K., Zhong, R., Darnell, R. B. & Burley, S. K. (1999) *Struct. Folding Des.* **7,** 191–203.
36. Lewis, H. A., Musunuru, K., Jensen, K. B., Edo, C., Chen, H., Darnell, R. B. & Burley, S. K. (2000) *Cell* **100,** 323–332.
37. Memili, E., Hong, Y.-K., Kim, D. K., Ontiveros, S. D. & Strauss, W. M. (2001) *Gene* **266,** 131–137.
38. Wolffe, A. P. & Matzke, M. A. (1999) *Science* **286,** 481–486.
39. Bird, A. P. & Wolffe, A. P. (1999) *Cell* **99,** 451–454.